Supporting Information

Realising the Electrochemical Stability of Graphene: Scalable Synthesis of an Ultra-durable Platinum Catalyst for the Oxygen Reduction Reaction

Gyen Ming A. Angel, Noramalina Mansor, Rhodri Jervis, Zahra Rana, Chris Gibbs, Andrew Seel, Alexander F.R. Kilpatrick, Paul R. Shearing, Christopher A. Howard, Dan J. L. Brett, Patrick L. Cullen**

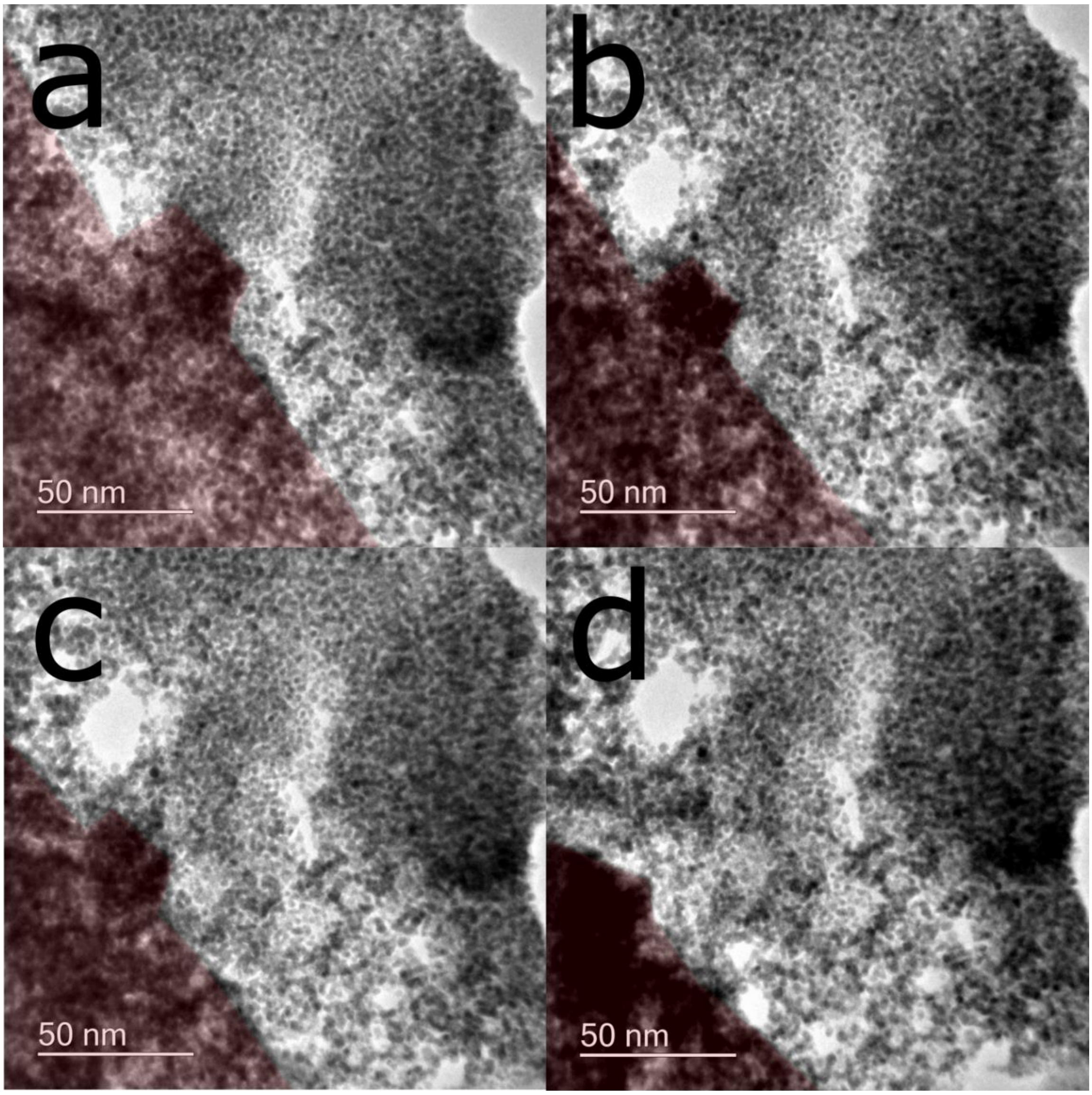

Figure S1 a,b,c,d sequential TEM images showing one sheet of GD-Pt/G (masked in red) moving over an underlying GD-Pt/G sheet in the electron beam

<u>Raman sample preparation:</u> $KC_{24}(NH_3)_{1.3}$ powder was loaded into a 1 mm borosilicate glass capillary within the glovebox, and then sealed with wax to ensure it remained air-free. Graphenide-derived platinum nanoparticle/graphene componsite (GD-Pt/G)

samples were obtained from solution via drop-casting onto glass slides which were then dried overnight in ambient conditions. All Raman spectra were obtained on a Renishaw InVia Microscope using a 488 nm laser and a 2400 l/mm diffraction grating. All spectra are normalised to the G-peak of each sample.

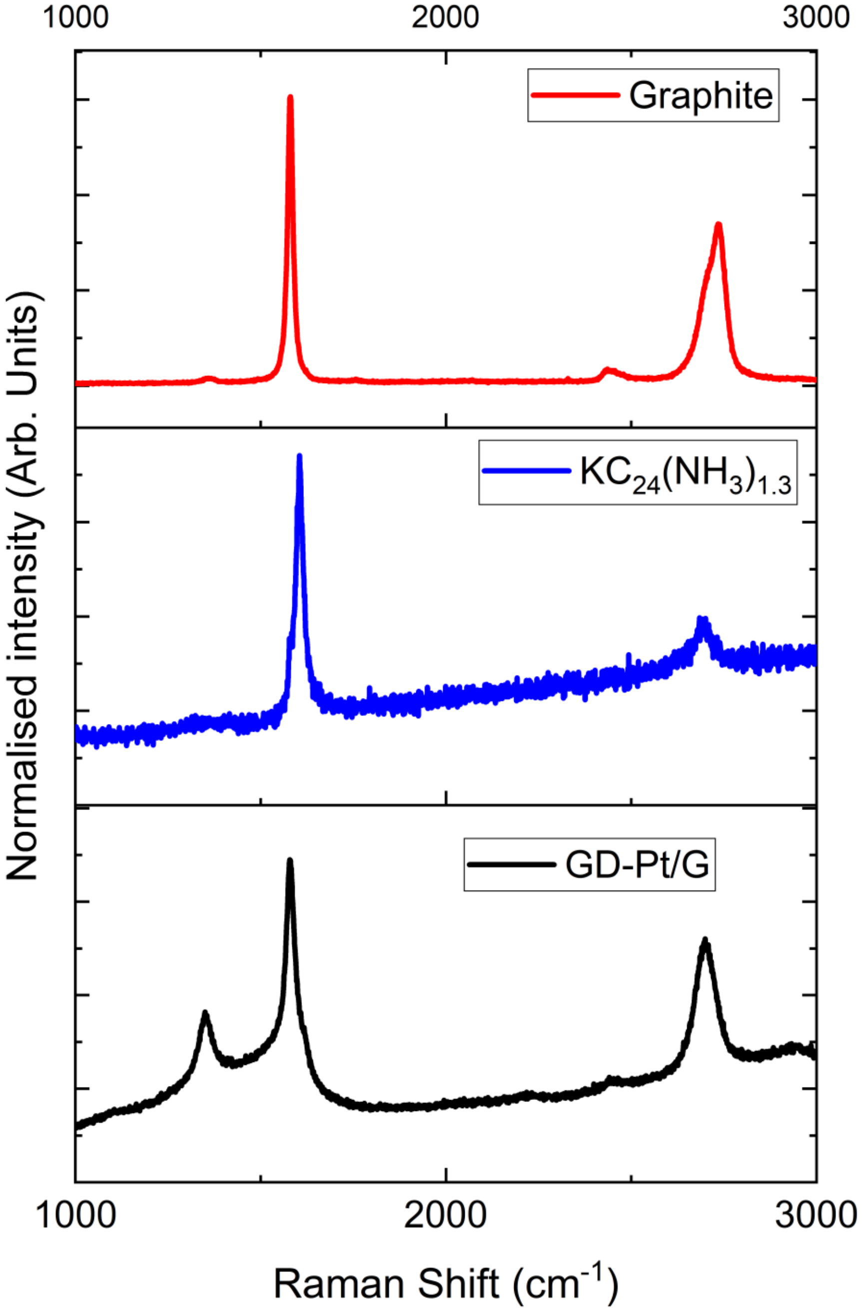

Figure S2 Raman spectra of the starting graphite, the $KC_{24}(NH_3)_{1.3}$ GIC and GD-Pt/G.

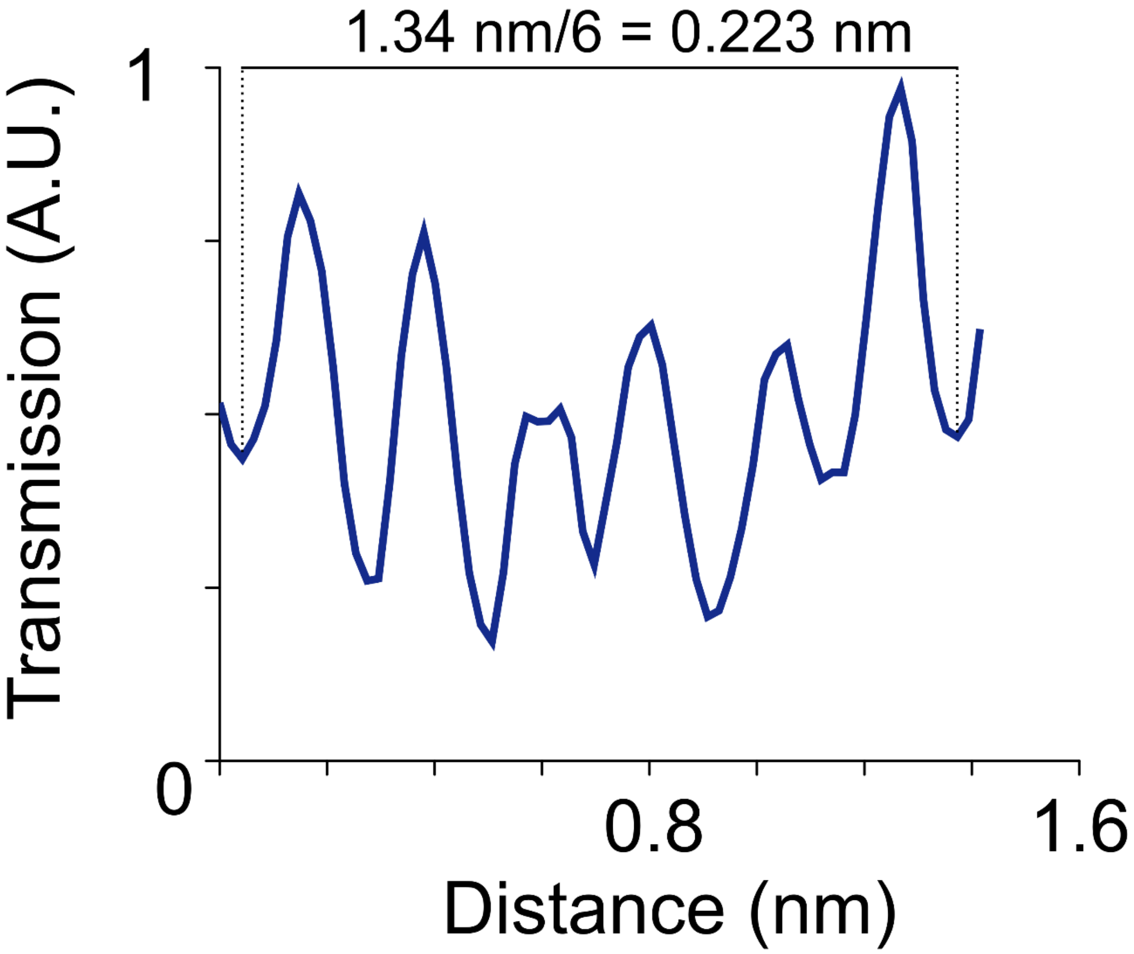

Figure S3 Line profile of platinum nanoparticle planes, visible in main text Figure 2a. The distance measured across seven planes was found to be ca. 1.34 nm, resulting in an interplanar distance of 0.223 nm. This corresponds with the (111) Pt interplanar spacing.

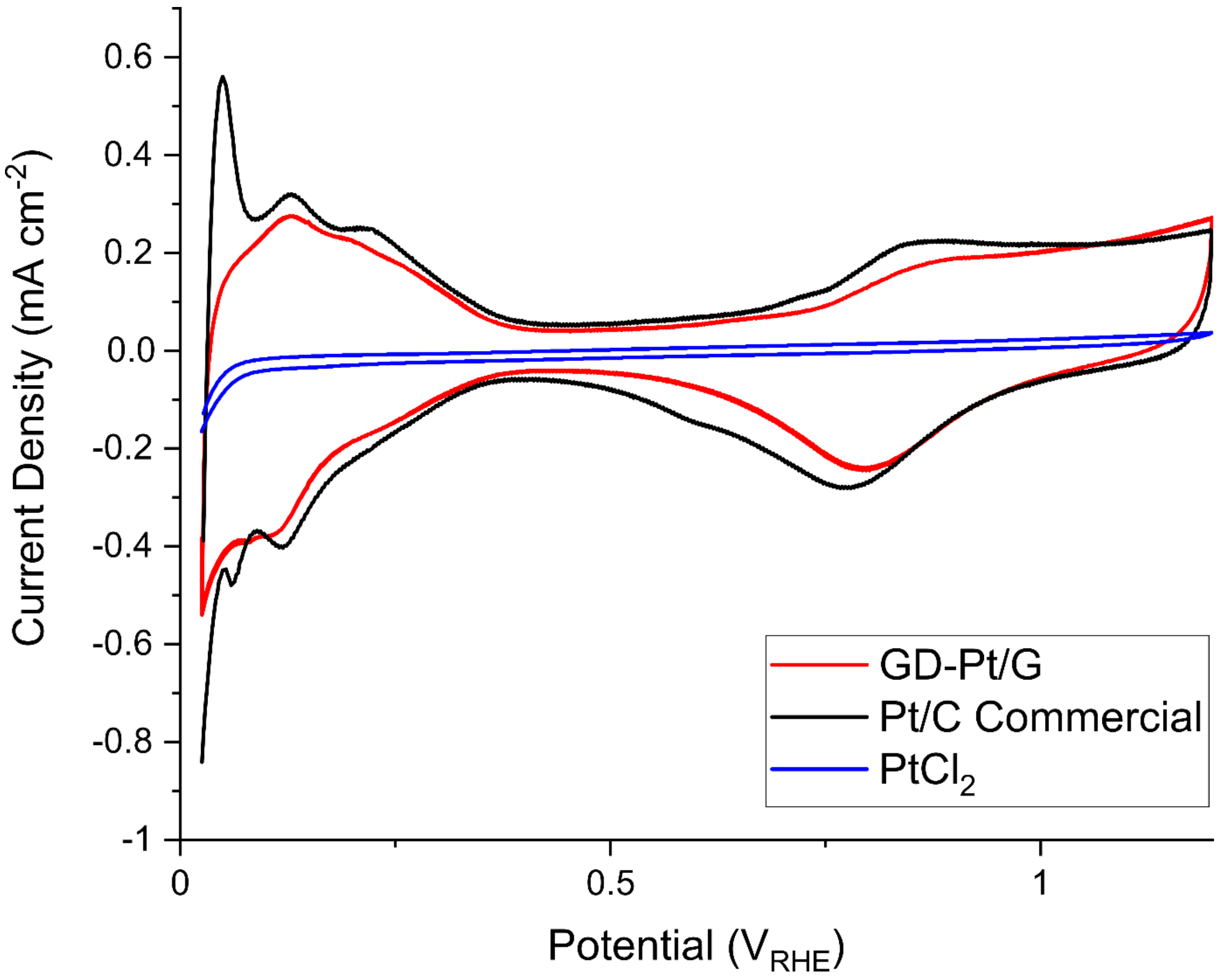

Figure S4 Cyclic voltammograms of GD-Pt/G and commercial Pt/C electrodes, in N_2 saturted 0.1M $HClO_4$, scan rate 20 mV s^{-1}.

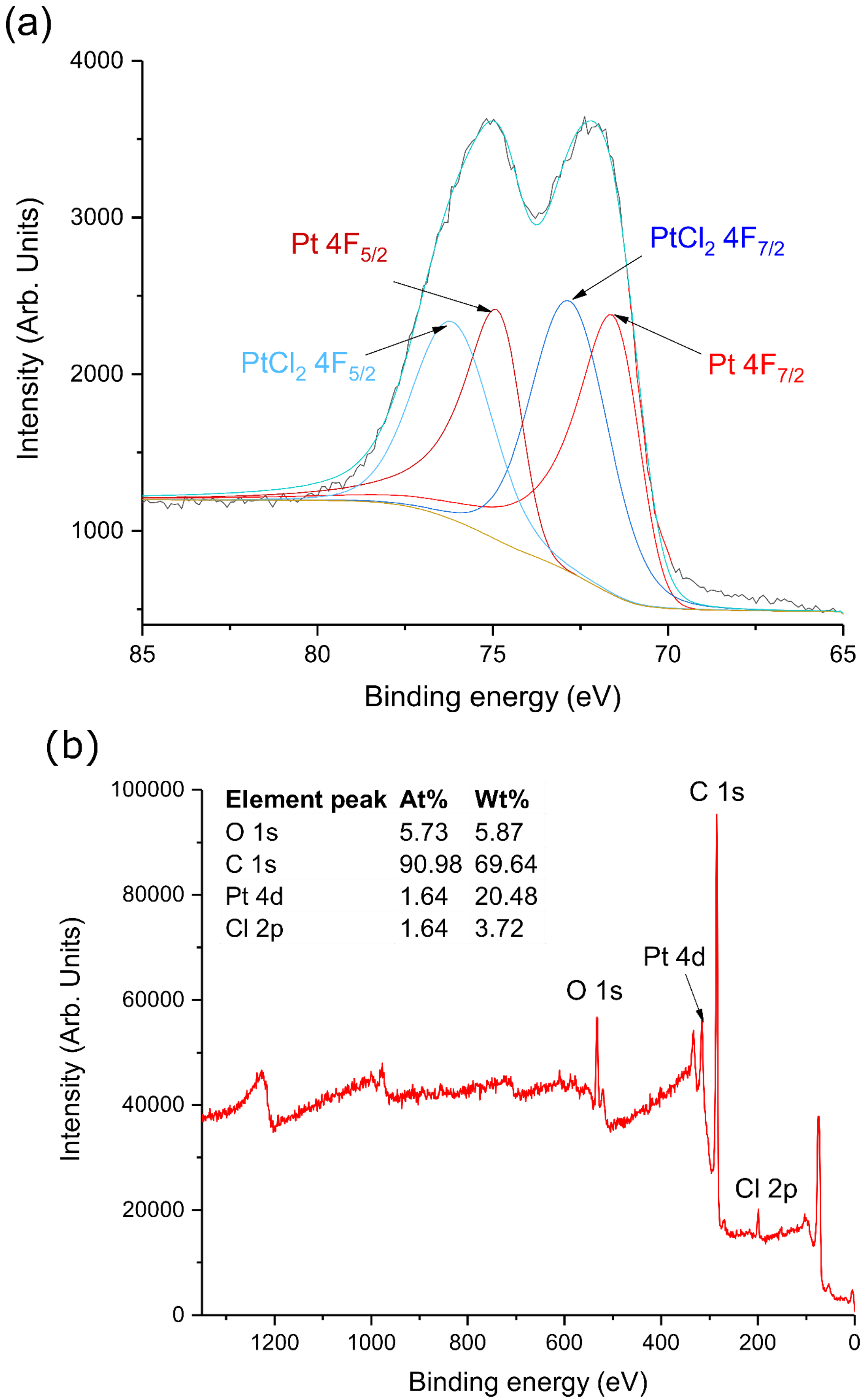

Element peak	**At%**	**Wt%**
O 1s	5.73	5.87
C 1s	90.98	69.64
Pt 4d	1.64	20.48
Cl 2p	1.64	3.72

Figure S5 (a) XPS high resolution scan of the Pt 4F region of GD-Pt/G powder. The peaks can be deconvoluted into a combination of platinum and platinum chloride peaks, with quantification suggesting a 50:50 mixture of platinum and unreacted platinum chloride, consistent with the At% obtained from the quantification of the survey XPS spectrum. **Figure S5 (b)** XPS Survey spectrum of GD-Pt/G powder with elemental quantification table inset. Quantification of the spectrum, used in combination with the high resolution Pt 4F scan, suggests that GD-Pt/G has a Pt loading weight of 11.5 wt%

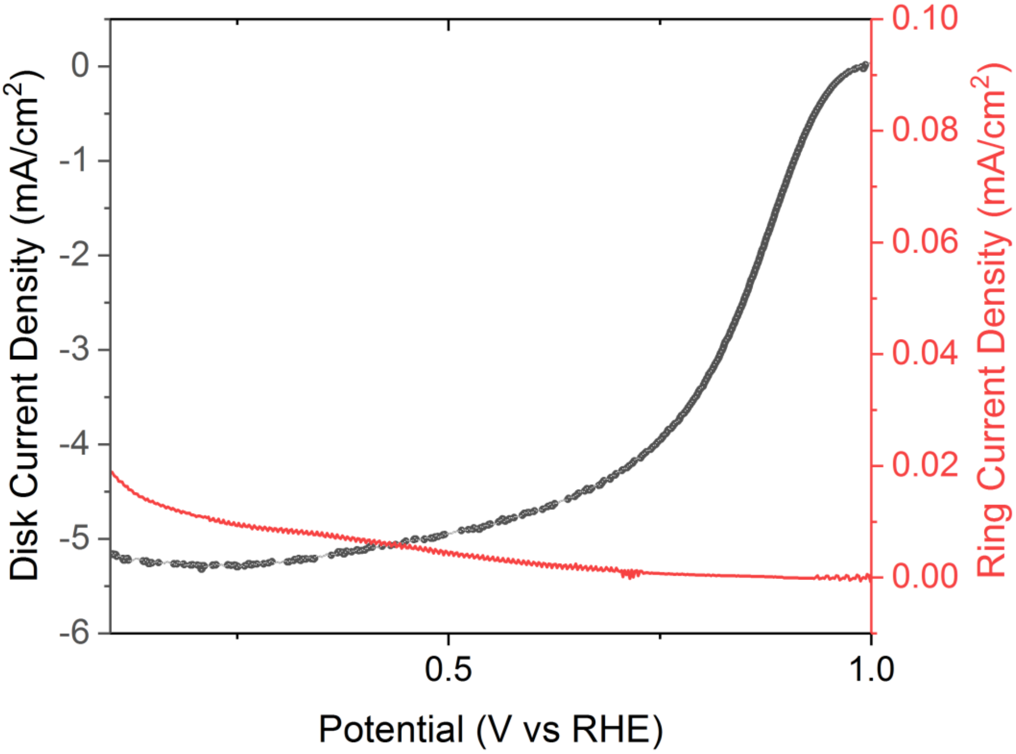

Figure S6 Linear sweep voltammogram obtained using a rotating ring-disk experiment for GD-Pt/G. This was performed in $HClO_4$ at a scan rate of 20 mV s^{-1}.

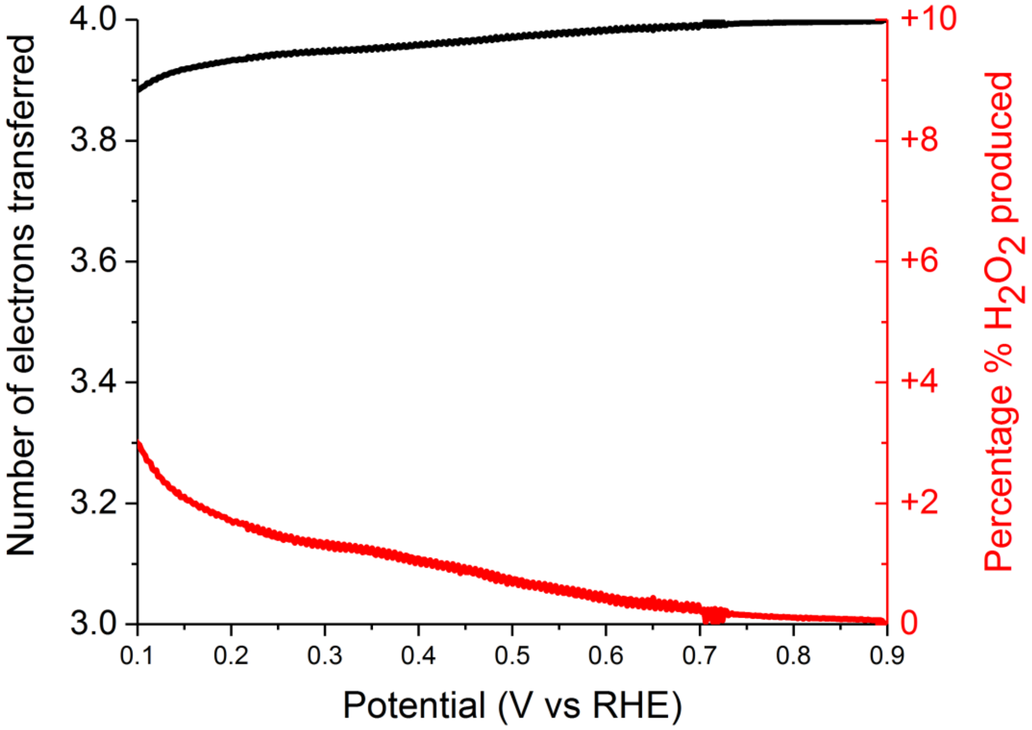

Figure S7 Number of electrons transferred and H_2O_2 yield calculated from Figure S6.

Summary of Department of Energy Accelerated Stress Test Protocols: The US Department of Energy has set out protocols and targets for accelerated stress tests of platinum catalyst layers in membrane electron assemblies, tested as part of a working fuel cell[1]. For testing the normal operating conditions of the fuel cell, the DoE protocol uses cyclic voltammograms scanned between 0.6-0.95 V_{RHE} for 30,000 cycles. To simulate the start-up and shut down of a fuel cell the test is modified to run between 1-1.5 V_{RHE} for 5000 cycles. However, for rotating disk electrode experiments, it has been found that to reliably reproduce trends in durability seen in full fuel cell stack tests, it is necessary to cycle between 1-1.6 $V_{RHE.}$[2] The accelerated stress tests performed in this work were run for 30,000 cycles in both cases. This is consistent with standard DoE protocol for the 0.6-1 V_{RHE} test, and go beyond the cycling requirements of the 1-1.6 V_{RHE} protocol.

	Catalyst	**Electrolyte**	**AST protocol**	**AST length**	**Stability**	**Pt/C Stability**
This work	GD-Pt/G	0.1 M HClO$_4$	0.6-1 V vs RHE, 100 mV/s	30,000 cycles	21 % in ECSA	30 % loss in ECSA
			1-1.6 V vs RHE, 100 mV/s	30,000 cycles	19 % loss in ECSA	50 % loss in ECSA
3	Pt/functionalised graphene	0.5M H$_2$SO$_4$	0.6 - 1V vs RHE, 50 mV/s	5000 cycles	37.6 % loss in ECSA	60 % loss in ECSA
4	FePt/rGO	0.1 M HClO$_4$	0.4 - 0.8 V vs Ag/AgCl, 100 mV/s	10,000 cycles	Almost no change in ORR activity	"Left shifted"
5	Ru/N-doped graphene	0.1 M HClO$_4$	0.6 - 1V vs RHE, 100mV/s	10,000 cycles	7 % decrease in limiting current, 18mV negative shift in half-wave potential	N.A.
			Chronoamperometric measurement at 0.7V vs RHE	10,000 s	10 % loss in current density at 0.7V vs RHE	38 % loss in current density at 0.7 V vs RHE
6	Au cluster/rGO	0.1 M KOH	Chronoamperometric measurement at -0.2 V vs Ag/AgCl	40,000 s	16% loss in current density at -0.2 V vs Ag/AgCl	50 % loss in current density at -0.2 V vs Ag/AgCl
7	Ag nanocrystals/rGO	0.1 M KOH	Potential window not specified, 50 mV/s	1000 cycles	15.6 % loss in ECSA	63.1 % loss in ECSA
8	Pd/rGO	0.1 M KOH	Chronoamperometric measurement at 0.63 V vs RHE	2000 s	ca. 93 % loss in current density at 0.63 V vs RHE	ca. 98 % loss in mass current density at 0.63 V vs RHE
			0.36 - 0.86 V vs RHE	4000 cycles	"little change in the ORR activity was observed"	N.A.
9	Pt/N-doped rGO	0.5 M H2SO$_4$	0.6 - 1.2 V vs RHE	4000 cycles	29.4 % loss in ECSA	80.8 % loss in ECSA
10	PtPd NPs/ rGO	0.1 M HClO$_4$	Chronoamperometric measurement at 0.1 V vs RHE	10,000 s	ca. 24 % loss in current density at 0.1 V vs RHE	ca. 48 % loss in current density at 0.1 V vs RHE
11	Pt/GO nanoribbons	0.1 M HClO$_4$	0.6 - 1 V vs RHE, 50 mV/s	10,000 cycles	65 % loss in ECSA	N.A.
12	PtPd nanocage/rGO	0.1 M HClO$_4$	0.6 - 1.05 V vs RHE, 50 mV/s	10,000 cycles	11.3 % loss in ECSA	N.A.
13	Cu-Pd/ rGO	0.1 M KOH	Neither potential window nor scan speed not specified	3000 cycles	8.8 % decrease in ORR limiting current	15.6 % decrease in ORR limiting current

14	Au clusters/ rGO	0.1 M KOH	-1 -0.2 V vs Ag/AgCl, 5 mV/s	1000 cycles	16 % loss in ECSA	27 % loss in ECSA
15	PtNi/rGo	0.5 M H_2SO_4	-0.2 - 1.2 V vs RHE, 50 mV/s	2000 cycles	96.6 % loss in ECSA	N.A.
16	PdPt@Pt/rGO	0.5 M H_2SO_4	Neither potential window nor scan speed not specified	1000 cycles	40 % loss in ECSA	N.A.
17	Pt/ carbon nanosheets	0.1 M $HClO_4$	0.46-0.96V vs RHE, 50 mV/s	5000 cycles	25 mV negative shift of half wave potential	36 mV negative shift of half wave potential
18	Au@Pt/rGO	0.1 M $HClO_4$	N.A. (single cell tests, no RDE ASTs)	N.A.	N.A.	N.A.
19	Pt/N-doped GO	0.1 M $HClO_4$	No durability tests	N.A.	N.A.	N.A.
20	Graphene capped Pt	0.1 M H_2SO_4	0.4-0.75 V vs Ag/AgCl, scan rate not specified	1000 cycles	No change in ECSA after 1000 cycles	N.A. Pt monolayer they grew themselves: ca. 45 % loss in ECSA
21	Pt/rGO/Carbon black	0.1 M $HClO_4$	0.6- 1.1 V vs RHE, scan rate not specified	20,000 cycles	5 % loss in ECSA	51 % loss in ECSA
22	Pt/Graphene nanoplatelets	1 M H_2SO_4	Chronoamperometric measurement at 1.2 V vs RHE	86,4000 s	35.4 % loss in current density	N.A.
23	FeNi/ N-doped rGO	0.5 M H_2SO_4	-0.2 – 1 V vs Ag/AgCl, 50 mV/s	1000 cycles	CVs shown but ECSA change not quantified	Bigger change in ECSA than for Pt/N-doped rGO
24	Co_3O_4 nanocrystals/ rGO	1 M KOH	Chronoamperometric measurement at 0.7 V vs RHE	25,000 s	0 % loss in current density at 0.7 V vs RHE	35 % loss in current density at 0.7 V vs RHE
25	Pt/SiC/rGO	0.1 M $HClO_4$	0.6-1.2 V vs RHE, scan rate not specified	10,000 cycles	59.7 % loss in ECSA	79.3 % loss in ECSA
26	Pt/rGO/carbon fiber	0.5 M H_2SO_4	-0.2-0.96 V vs SCE, 50 mV/s	1500 cycles	81.9 % loss in ECSA	86.4 % loss in ECSA
27	Pt/rGO	0.1 M $HClO_4$	0-1.2 V vs RHE, scan rate not specified	10,000 cycles	68 % loss in ECSA	N.A.
28	Pd/N-carbon nanosheet	0.1 M KOH	Chronoamperometric measuerment at 0.6 V vs RHE	35,000 s	20 % loss in current density at 0.6 V vs RHE	33 % loss in current density at 0.6 V vs RHE
29	Cu/N-rGO	0.1 M KOH	Chronoamperometric measurement at 0.7 V vs RHE	1200s	Ca. 0% loss in current density at 0.7 V vs RHE	Ca. 50 % loss in current density at 0.7V vs RHE

30	Rh/rGO	0.1 M KOH	Chronoamperometric measurement at unspecified potential	25,000s	10.9 % loss in current density	47.5 % loss in current density
31	Fe@PANI/rGO	0.1 M KOH	0.2 – 1.2 V vs RHE, 50 mV/s	10,000 cycles	13 mV decrease in $E_{1/2}$	82 mV decrease in $E_{1/2}$
32	Pt/N-rGO + carbon nanospheres	0.1 M $HClO_4$	0.5 – 1 V vs RHE, scan rate not specified	5000 cycles	6% loss in ECSA	40.2 % loss in ECSA
33	Pt/N-doped TiO_2 + N-doped rGO	0.5 M H_2SO_4	1 - 1.5 V vs RHE, 500 mV/s scan rate	20,000 cycles	16.9% loss in ECSA	40.1% loss in ECSA
34	Ti/Pt-Pd/ Graphene nanoribbons	0.1 M $HClO_4$	0.4 – 1.0 V vs RHE, 1 V/s	10,800 cycles	ECSA “does not vary”	6 % loss in ECSA
			1 – 1.5 V vs RHE, 500 mV/s	5000 cycles	9.7 % loss in ECSA	N.A.
35	Pt/coiled carbon nanosheets	0.5 M H_2SO_4	Chronoamperometric measurement at 0.68 V vs RHE	3500 s	Ca. 85% loss in current density measured at 0.68 V vs RHE	Ca. 100% loss in current density measured at 0.68 V vs RHE
36	Pt@MoS_2/N-rGO	0.5 M H_2SO_4	0.6 – 1.0 V vs RHE, 100 mV/s	30,000 cycles	23.06 % loss in ECSA	28.02 % loss in ECSA
37	Pt single atoms/rGO	0.1 M KOH	0.4 – 1.0 V vs RHE, 50 mV/s	2000 cycles	0.025 V negative shift in $E_{1/2}$	N.A.
38	Pt/ graphene-like 3D carbon	0.5 M H_2SO_4	Chronopotentiometry at -3.016 mA/cm^2	7200 s	10 % decrease in mass activity at 0.8 V vs RHE	39.2 % decrease in mass activity at 0.8 V vs RHE
39	Pt/graphene	0.1 M $HClO_4$	0.6 - 1 V, 100 mV/s, followed by 0.6 – 1.5 V,	18,000 cycles, followed by 800 cycles	5% loss in ECSA, followed by a further 20% loss	40% loss in ECSA followed by a further 22% loss
40	Ag/N-doped graphene	0.1 M $HClO_4$	-0.1 – 1 V, 50 mV/s	10,000 cycles	22 mV negative shift in $E_{1/2}$	86 mV negative shift in $E_{1/2}$
41	Pt/ N-doped rGO foam	0.5 M H_2SO_4	Chronoamperometric measurement at 0.6 V vs RHE	30,000 s	14.4 % decrease in current density measured at 0.6 V vs RHE	33.1 % decrease in current density measured at 0.6 V vs RHE
			0.05 – 1.2 V vs RHE, 50 mV/s	10,000 cycles	24 mV negative shift in $E_{1/2}$	75 mV negative shift in $E_{1/2}$
42	$Ag_4Bi_2O_5/MnO_x$ - rGO	0.1 M KOH	Chronoamperometric measurement at 0.03 V vs Hg/HgO	10,800 s	14 % decrease in current density	42 % decrease in current density

					measured at 0.03 V vs Hg/HgO	measured at 0.03 V vs Hg/HgO
43	Cu/N-doped rGO	0.1 M KOH	Chronoamperometric measurement at 0.7 V vs RHE	25,000 s	4 % decrease in current density measured at 0.7 V vs RHE	19.5 % decrease in current density measured at 0.7 V5 vs RHE
44	$Pt/IrO_2Nb_2O_5$ - rGO	0.5 M H_2SO_4	0.0 – 1.2 V vs RHE, 50 mV/s	2000 cycles	23.8 % loss in ECSA	39.4 loss in ECSA
45	Fe-doped mayenite/rGO	0.1 M KOH	Chronoamperometric measurement at 0.87 V vs RHE	39,600 s	Current density “almost remains the same”	40 % decrease in current density measured at 0.87 V vs RHE
46	Pt-Pd-Cu/graphene nanoribbon	0.1 M $HClO_4$	0.6 – 1 V vs RHE, 50 mV/s	10,000 cycles	Ca. 30 % decrease in mass activity	N.A.
47	Mn doped CeO_2/rGO	0.1 M KOH	Chronoamperometric measurement at -0.35 V vs Ag/AgCl	12,500 cycles	20 % decrease in current density measured at-0.35 V vs Ag/AgCl	40% decrease in current density measured at-0.35 V vs Ag/AgCl
48	Fe-N-CNT/rGO	0.1 M KOH	Chronoamperometric measurement at 0.8 V vs RHE	72,000 s	6 % decrease in current density measured at 0.8 V vs RHE	29 % decrease in current density measured at 0.8 V vs RHE
49	Pt/B-rGO	0.1 M KOH	0.57 – 1.17 V vs RHE, scan rate not specified	6000 cycles	Onset and half wave potential “close to initial cycle”	N.A.
50	Pt/rGO + CNT spacers	0.5 M H_2SO_4	0 – 1.2 V vs RHE, 50 mV/s	2000 cycles	39 % loss in ECSA	19% loss in ECSA
51	ZIF-N-rGO porous nanosheets	0.1 M KOH	Chronoamperometric measurement at -0.4 V vs Ag/AgCl	28,000 s	6 % decrease in current density measured at -0.4 V vs Ag/AgCl	20 % decrease in ECSA measured at -0.4 V vs Ag/AgCl
52	Fe-N-C microspheres	0.1 M KOH	0.55 – 0.95 V vs RHE, 100 mV/s	10,000 cycles	29 mV negative shift in $E_{1/2}$	31 mV negative shift in $E_{1/2}$

Table S1 | To the best of our knowledge, a review of graphene supported catalysts for ORR, their associated accelerated stress test protocols and results.

This work: GD-Pt/G				
0.6 - 1V_{RHE}				
Number of cycles	Limiting current density (mA cm^{-2})	Change in limiting current (mA cm^{-2})	Half wave potential (mV_{RHE})	Half wave potential shift (mV)
0	5.71	0	894	0
30,000	5.58	-0.13	876	-18
1 - 1.6V_{RHE}				
0	5.23	0	865	0
30,000	4.92	-0.31	850	-15
Commercial Pt/C				
0.6 - 1V_{RHE}				
Number of cycles	Limiting current density (mA cm^{-2})	Change in limiting current (mA cm^{-2})	Half wave potential (mV_{RHE})	Half wave potential shift (mV)
0	5.84	0	836	0
30,000	5.7	-0.14	874	38
1 - 1.6V_{RHE}				
0	6.06	0	892	0
30,000	5.49	-0.57	822	-70

Table S2│ Limiting current density , half wave potential and relative changes after 30,000 cycles for both GD-Pt/G and the commercial Pt/C in the 0.6 – 1 V_{RHE} and 1 - 1.6 V_{RHE} potential ranges.

1 Fuel cell Technologies Office: Multi-year Research, Development and Demonstration Plan, https://www.energy.gov/sites/prod/files/2017/05/f34/fcto_myrdd_fuel_cells.pdf, (accessed 18 January 2019).

2 A. Riese, D. Banham, S. Ye and X. Sun, *J. Electrochem. Soc.*, 2015, **162**, F783–F788.

3 R. Kou, Y. Shao, D. Wang, M. H. Engelhard, J. H. Kwak, J. Wang, V. V. Viswanathan, C. Wang, Y. Lin, Y. Wang, I. A. Aksay and J. Liu, *Electrochem. commun.*, 2009, **11**, 954–957.

4 S. Guo and S. Sun, *J. Am. Chem. Soc.*, 2012, **134**, 2492–2495.

5 C. Zhang, J. Sha, H. Fei, M. Liu, S. Yazdi, J. Zhang, Q. Zhong, X. Zou, N. Zhao, H. Yu, Z. Jiang, E. Ringe, B. I. Yakobson, J. Dong, D. Chen and J. M. Tour, *ACS Nano*, 2017, **11**, 6930–6941.

6 H. Yin, H. Tang, D. Wang, Y. Gao and Z. Tang, *ACS Nano*, 2012, **6**, 8288–8297.

7 M. S. Ahmed, D.-W. Lee and Y.-B. Kim, *J. Electrochem. Soc.*, 2016, **163**, F1169–F1176.

8 Y.-X. Huang, J.-F. Xie, X. Zhang, L. Xiong and H.-Q. Yu, *ACS Appl. Mater. Interfaces*, 2014, **6**, 15795–15801.

9 D. He, Y. Jiang, H. Lv, M. Pan and S. Mu, *Appl. Catal. B Environ.*, 2013, **132–133**, 379–388.

10 L. Sun, H. Wang, K. Eid, S. M. Alshehri, V. Malgras, Y. Yamauchi and L. Wang, *Electrochim. Acta*, 2016, **188**, 845–851.

11 G. V. Fortunato, F. De Lima and G. Maia, *J. Power Sources*, 2016, **302**, 247–258.

12 S. Bai, C. Wang, W. Jiang, N. Du, J. Li, J. Du, R. Long, Z. Li and Y. Xiong, *Nano*

Res., 2015, **8**, 2789–2799.

13 Y. Zheng, S. Zhao, S. Liu, H. Yin, Y. Y. Chen, J. Bao, M. Han and Z. Dai, *ACS Appl. Mater. Interfaces*, 2015, **7**, 5347–5357.

14 S. Xu and P. Wu, *J. Mater. Chem. A*, 2014, **2**, 13682–13690.

15 W. kyo Suh, P. Ganesan, B. Son, H. Kim and S. Shanmugam, *Int. J. Hydrogen Energy*, 2016, **41**, 12983–12994.

16 S. S. Li, J. J. Lv, L. N. Teng, A. J. Wang, J. R. Chen and J. J. Feng, *ACS Appl. Mater. Interfaces*, 2014, **6**, 10549–10555.

17 L. Zeng, X. Cui and J. Shi, *Sci. China Mater.*, 2018, 1–10.

18 N. Seselj, C. Engelbrekt, Y. Ding, H. A. Hjuler and J. Ulstrup, *Adv. Energy Mater.*, 2018, **1702609**, 1–12.

19 zoltan konya Tamas Varga, Agnes Timea Varga, Gergo Ballai, Henrik haspel, Akos Kukovecz, *Carbon N. Y.*, 2018, **133**, 90–100.

20 A. Abdelhafiz, A. Vitale and P. Buntin, *Energy Environ. Sci.*, 2018, **11**, 1610–1616.

21 Y. Y. Li, Y. Y. Li, E. Zhu, T. McLouth, C. Y. Chiu, X. Huang and Y. Huang, *J. Am. Chem. Soc.*, 2012, **134**, 12326–12329.

22 E. Daş, S. Alkan Gürsel, L. Işıkel Şanlı and A. Bayrakçeken Yurtcan, *Int. J. Hydrogen Energy*, 2017, **42**, 19246–19256.

23 N. A. M. Barakat, A. G. El-Deen, Z. K. Ghouri and S. Al-Meer, *Sci. Rep.*, 2018, **8**, 1–11.

24 Y. Liang, Y. Li, H. Wang, J. Zhou, J. Wang, T. Regier and H. Dai, *Nat. Mater.*, 2011, **10**, 780–786.

25 X. Chen, D. He, H. Wu, X. Zhao, J. Zhang, K. Cheng, P. Wu and S. Mu, *Sci. Rep.*, 2015, **5**, 1–10.

26 X. Mu, Z. Xu, Y. Ma, Y. Xie, H. Mi and J. Ma, *Electrochim. Acta*, 2017, **253**, 171–177.

27 P. Zhang, W. Tu, R. Wang, S. Cai, J. Wu, Q. Yan, H. Pan, H. Zhang and H. Tang, *Int. J. Electrochem. Sci.*, 2016, **11**, 10763–10778.

28 S. Zhang, L. Wang, L. Fang, Y. Tian, Y. Tang, X. Niu, Y. Hao and Z. Li, *J. Electrochem. Soc.*, 2020, **167**, 054508.

29 X. Wen, H. Qi, Y. Cheng, Q. Zhang, C. Hou and J. Guan, *Chinese J. Chem.*, 2020, cjoc.202000073.

30 M. Sookhakian, G. B. Tong and Y. Alias, *Appl. Organomet. Chem.*, 2020, **34**, 1–11.

31 M. S. Ahmed, H. Begum and Y. B. Kim, *J. Power Sources*, 2020, **451**, 227733.

32 Y. Xiong, M. You, F. Liu, M. Wu, C. Cai, L. Ding, C. Zhou, M. Hu, W. Deng and S. Wang, *ACS Appl. Energy Mater.*, 2020, **3**, 2490–2495.

33 C. Park, E. Lee, G. Lee and Y. Tak, *Appl. Catal. B Environ.*, 2020, **268**, 118414.

34 G. V. Fortunato, E. S. F. Cardoso, B. K. Martini and G. Maia, *ChemElectroChem*, 2020, **7**, 1610–1618.

35 Z. Tong, M. Wen, C. Lv, Q. Zhang, Y. Yin, X. Liu, Y. Li, C. Liao, Z. Wu and D. D. Dionysiou, *Appl. Catal. B Environ.*, 2020, **269**, 118764.

36 S. Ramakrishnan, M. Karuppannan, M. Vinothkannan, K. Ramachandran, O. J. Kwon and D. J. Yoo, *ACS Appl. Mater. Interfaces*, 2019, **11**, 12504–12515.

37 X. Song, N. Li, H. Zhang, H. Wang, L. Wang and Z. Bian, *J. Power Sources*, 2019, **435**, 226771.

38 Y. Kim, D. Lee, Y. Kwon, T. W. Kim, K. Kim and H. J. Kim, *J. Electroanal. Chem.*, 2019, **838**, 89–93.

39 E. Bertin, A. Münzer, S. Reichenberger, R. Streubel, T. Vinnay, H. Wiggers, C. Schulz, S. Barcikowski and G. Marzun, *Appl. Surf. Sci.*, 2019, **467**–**468**, 1181–1186.

40 Y. Yan, S. Yan, Z. Yu and Z. Zou, *ChemCatChem*, 2019, **11**, 1033–1038.

41 K. K. Karuppanan, A. V. Raghu, M. K. Panthalingal, V. Thiruvenkatam, P. Karthikeyan and B. Pullithadathil, *Sustain. Energy Fuels*, 2019, **3**, 996–1011.

42 J. Wang, J. Pan, X. Zeng, G. Tang, J. Cai, A. Khan, Y. Sun and X. Liu, *J. Solid State Electrochem.*, 2019, **23**, 2737–2746.

43 L. Bai, C. Hou, X. Wen and J. Guan, *ACS Appl. Energy Mater.*, 2019, **2**, 4755–4762.

44 F. D. Kong, L. J. Yang, J. Liu, A. X. Ling, M. J. Shi, M. Lv, Z. Q. Xu, Y. L. Niu and H. Y. Wang, *Catal. Letters*, 2019, **149**, 3041–3047.

45 K. Khan, A. K. Tareen, M. Aslam, S. Ali Khan, Q. khan, Q. U. Khan, M. Saeed, A. Siddique Saleemi, M. Kiani, Z. Ouyang, H. Zhang and Z. Guo, *Sci. Rep.*, 2019, **9**, 1–11.

46 C. V. Boone and G. Maia, *Electrochim. Acta*, 2019, **303**, 192–203.

47 I. Hota, S. Soren, B. D. Mohapatra, A. K. Debnath, K. P. Muthe, K. S. K. Varadwaj and P. Parhi, *J. Electroanal. Chem.*, 2019, **851**, 113480.

48 Y. Zheng, F. He, J. Wu, D. Ma, H. Fan, S. Zhu, X. Li, Y. Lu, Q. Liu and X. Hu, *ACS Appl. Nano Mater.*, 2019, **2**, 3538–3547.

49 D. Lim, Y. Shim, J. Oh, S. Kim and S. Park, *J. Solid State Chem.*, 2019, **271**, 168–174.

50 Z. Liu, A. A. Abdelhafiz, Y. Jiang, C. Qu, I. Chang, J. Zeng, S. Liao and F. M. Alamgir, *Mater. Chem. Phys.*, 2019, **225**, 371–378.

51 H. X. Zhong, J. Wang, Y. W. Zhang, W. L. Xu, W. Xing, D. Xu, Y. F. Zhang and X. B. Zhang, *Angew. Chemie - Int. Ed.*, 2014, **53**, 14235–14239.

52 F. L. Meng, Z. L. Wang, H. X. Zhong, J. Wang, J. M. Yan and X. B. Zhang, *Adv. Mater.*, 2016, **28**, 7948–7955.